CRB based-design of linear antenna arrays for near-field source localization

Houcem Gazzah, Jean-Pierre Delmas

CRB Based-Design of Linear Antenna Arrays for Near-Field Source Localization

Houcem Gazzah and Jean Pierre Delmas

Abstract

This paper is devoted to the Cramer Rao bound (CRB) on the angle and range of a narrow-band near-field source localized by means of an arbitrary linear array using the exact expression of the time delay parameter. First, we prove that the conditional and unconditional CRBs are proportional for an arbitrary parametrization of the steering vector. Then, a Taylor expansion of the CRB is conducted to obtain accurate non-matrix closed-form expressions of the CRB on angle and range. In contrast to the existing expressions, our expressions are simple, interpretable and more general because the sensors are only constrained to be placed along some axis. Our analysis leads to the characterization of a class of *centro-symmetric* linear arrays with better near-field angle and range estimation capabilities.

Index Terms

Cramer Rao bounds, linear antenna arrays, direction-of-arrival and range estimation, near-field source localization.

I. Introduction

Uniform linear arrays (ULA) are the most commonly used type of linear antenna arrays because they are ambiguity-free and allow for fast algorithms, when direction of arrival (DOA) estimation of far-field sources is sought. However, when the source is located in the antenna near-field, a change of the signal model occurs as a new parameter is to be considered: the source-to-antenna distance. Fast algorithms are no longer applicable, and, more seriously, the new (range) parameter will affect DOA estimation accuracy, and, for some applications, is itself of interest and needs to be estimated. In this context, we

Houcem Gazzah is with the Department of Electrical and Computer Engineering, University of Sharjah, 27272, UAE. E-mail: hgazzah@sharjah.ac.ae, Tel.: (971) 6.5050.917, Fax.: (971) 6.5050.872. Jean-Pierre Delmas is with Telecom SudParis, Departement CITI, CNRS UMR 5157, Evry, France. E-mail: jean-pierre.delmas@it-sudparis.eu.

prove that the ULA configuration is not the best choice. Alternative (other than uniform) placement of the array sensors is shown to improve range estimation.

To motivate our design, we study the algorithm-independent CRB which constitutes the minimum achievable variance on the estimated source parameters, here DOA and range of the near-field source. Despite the huge literature about DOA estimation [1], research has been mostly dedicated to far-field sources. In fact, when the source is in the array far-field, the (planar) waveform reaches two sensors with a time difference that is proportional to the spacing between the two sensors. Hence, it is possible to obtain simple and interpretable non-matrix expressions for the CRB (see e.g., [2]). In contrast, when the source is in the antenna near-field, the time delay expression is more intricate and only approximate non-matrix expressions of this CRB can be obtained. Inspired by subspace-based DOA algorithms, early ones were based on an approximate propagation model based on second-order Taylor expansion of the time delay parameter [3], [4]. Only lately has the exact time delay formula been used [5], but restricted to the ULA.

We start by proving a fact about the so-called conditional and unconditional CRBs. Often, they have been considered as independent (see e.g., the recent papers [15] and [5] which even concludes by "extension of this work for stochastic sources is under consideration"). In this paper, we show that they are, actually, proportional, an issue previously overlooked. Then, we investigate accurate non-matrix expressions of the CRB on both DOA and range, using linear arrays of arbitrarily spaced sensors. They are more general than those of [5] because we do not assume uniform linear arrays (neither punctured nor sparse) where inter-sensor spacings[1] are multiples of a minimum distance [7]. They are also more compact than those from [4], [5] and [6] if applied to the special case of ULA, and so thanks to a different coordinate system that implies a different definition of DOA and range.

The obtained CRB expressions allow for a rich interpretation of the array estimation capabilities when the source is in the antenna near-field. For instance, they highlight the interest of a class of *centro-symmetric* linear arrays made of pairs of sensors symmetrically located along the two sides of the linear antenna array. Attractive features of such centro-symmetric linear arrays include lower DOA and range CRBs and faster convergence to the lower far-field DOA CRB. Also, we show that within centro-symmetric linear arrays, ULA is not the best choice. Centro-symmetric linear arrays can be found that have identical DOA CRB as the ULA but significantly lower range CRB (by as much as 50%).

[1]Constraints on the array positions, often adopted to limit array ambiguities [8], may, at the same time, affect estimation performance [9].

In fact, a geometric parameter is identified that controls the near-field estimation performance of the centro-symmetric linear array.

The paper is organized as follows. Sec. II formulates the problem and specifies the data model. Sec. III is dedicated to new expressions of the CRB. First, assuming an arbitrary parametrization of the steering vector, we prove that the conditional and unconditional CRB are proportional. Then, we focus on the DOA and range estimation of near-field sources. Using Taylor expansion, new expressions of the CRB are derived, and numerically validated. The important class of centro-symmetric arrays is studied in details in Sec. IV where better-than-ULA are obtained. This paper is concluded in Sec. V.

II. Data Model

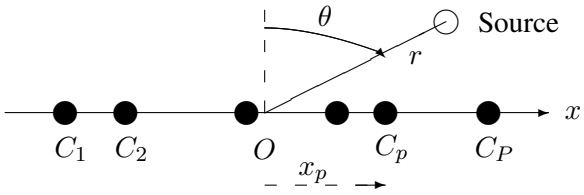

Fig. 1. Source in the near-field of the arbitrary linear array.

As depicted in Fig. 1, we consider a linear antenna array made of P sensors $C_1, \cdots, C_P$. They are located along a straight line at coordinates $x_1, \cdots, x_P$, respectively. Without loss of generality, we assume the array centroid to be at the origin O of this axis. This choice will also allow for more compact expressions of the CRB, compared to [4], [5]. A narrow-band signal $s(t)$, with wavelength λ, is emitted towards the antenna array by a source S located at a range r from the origin O and forming an angle θ w.r.t. the normal of the array. The snapshot collected by sensor p at time index t is

$$y_p(t) = g_p \exp\left(i\tau_p\right) s(t) + n_p(t), \tag{1}$$

where $s(t)$ and $n_p(t)$ represent, respectively, the source signal collected at the origin and the ambient additive noise collected by sensor p. Amplitude g_p may depend on both r and θ, while τ_p is defined as $\tau_p = 2\pi(SO - SC_p)/\lambda$, which can be rewritten as

$$\tau_p = 2\pi\frac{r}{\lambda}\left(1 - \sqrt{\beta_p}\right)$$

with $\beta_p \overset{\text{def}}{=} 1 - 2\frac{x_p}{r}\sin(\theta) + \frac{x_p^2}{r^2}$. Based on N snapshots $\{y_p(t)\}_{p=1,\ldots,P;t=t_1,\ldots,t_N}$, estimates of both the range r and the DOA θ are obtained using a variety of algorithms, among which a few are capable of achieving the stochastic CRB [10].

Estimation accuracy is evaluated in terms of the CRB, for which the usual statistical properties about $n_p(t)$ and $s(t)$ are the following: (i) $n_p(t)$ and $s(t)$ are independent, (ii) $\{n_p(t)\}_{p=1,...,P;t=t_1,...,t_N}$ are independent, zero-mean circular Gaussian distributed with variance σ_n^2, (iii) $\{s(t)\}_{t=t_1,...,t_N}$ are assumed to be either deterministic unknown parameters (the so-called conditional or deterministic model), or independent zero-mean circular Gaussian distributed with variance σ_s^2 (the so-called unconditional or stochastic model).

III. Expressions of the CRB

A. A general result about the CRB

We prove that the stochastic and deterministic CRBs are equal, up to a multiplicative constant, in the specific case of a single source. Let's, first, consider an arbitrary number K of sources (with $K < P$) with an arbitrary parametrization $\boldsymbol{\alpha} = [\alpha_1, ..., \alpha_L]^T$ of the steering vectors $\mathbf{a}(\boldsymbol{\alpha})$ related to array geometry or polarization, defined by

$$[\mathbf{a}(\boldsymbol{\alpha})]_{p=1,..,P} = g_p e^{i\tau_p},$$

where g_p and τ_p denote the gain and the delay of the p-th sensor w.r.t. the origin O. g_p includes in particular possible power profiles and/or directional gains. General compact expressions of the CRB, concentrated on the parameters of the K steering vectors alone, have been derived for these two models of sources (see e.g., [13]) for one parameter per source. The expression of the stochastic CRB has been extended for several parameters per source in [14, Appendix D], and following the proof given in [13], the expression of the deterministic CRB can be also extended to several parameters per source. These expressions are given respectively by

$$\mathrm{CRB}_{\mathrm{sto}}(\boldsymbol{\alpha}) = \frac{\sigma_n^2}{2N}\left[\mathrm{Re}\left(\mathbf{H} \odot ((\mathbf{R}_s \mathbf{A}^H \mathbf{R}_y^{-1} \mathbf{A} \mathbf{R}_s)^T \otimes \mathbf{1}_L)\right)\right]^{-1} \quad (2)$$

$$\mathrm{CRB}_{\mathrm{det}}(\boldsymbol{\alpha}) = \frac{\sigma_n^2}{2N}\left[\mathrm{Re}\left(\mathbf{H} \odot (\mathbf{R}_s^T \otimes \mathbf{1}_L)\right)\right]^{-1}, \quad (3)$$

where $\mathbf{R}_y \overset{\mathrm{def}}{=} \mathrm{E}[\mathbf{y}(t)\mathbf{y}^H(t)]$ with $\mathbf{y}(t) \overset{\mathrm{def}}{=} [y_1(t), ..., y_P(t)]^T$, $\mathbf{R}_s \overset{\mathrm{def}}{=} \mathrm{E}[\mathbf{s}(t)\mathbf{s}^H(t)]$ with $\mathbf{s}(t) \overset{\mathrm{def}}{=} [s_1(t), ..., s_K(t)]^T$ in (2) and $\mathbf{R}_s \overset{\mathrm{def}}{=} \frac{1}{N}\sum_{n=1}^N \mathbf{s}(t_n)\mathbf{s}^H(t_n)]$ in (3), $\mathbf{A} \overset{\mathrm{def}}{=} [\mathbf{a}_1, ..., \mathbf{a}_K]$ with $\mathbf{a}_k$ is the steering vector of the k-th source parameterized by $\boldsymbol{\alpha}_k \in \mathbb{R}^L$, $\mathbf{H} \overset{\mathrm{def}}{=} \mathbf{D}^H\left[\mathbf{I} - \mathbf{A}(\mathbf{A}^H\mathbf{A})^{-1}\mathbf{A}^H\right]\mathbf{D}$ and $\mathbf{D} \overset{\mathrm{def}}{=} [\frac{d\mathbf{a}_1}{d\boldsymbol{\alpha}_1}, ..., \frac{d\mathbf{a}_K}{d\boldsymbol{\alpha}_K}]$, and where $\otimes$, $\odot$ and $\mathbf{1}_L$ are the Kronecker product, the Hadamard product and the $L \times L$ matrix of 1s, respectively.

Specialized to a single source for which $\mathbf{R}_y = \sigma_s^2 \mathbf{a}(\boldsymbol{\alpha})\mathbf{a}^H(\boldsymbol{\alpha}) + \sigma_n^2 \mathbf{I}$ where $\sigma_s^2 \stackrel{\text{def}}{=} \frac{1}{N}\sum_{n=1}^{N} |s(t_n)^2|$ for the deterministic model of the source, it is straightforward to prove the following result

$$\text{CRB}_{\text{sto}}(\boldsymbol{\alpha}) = \left(1 + \frac{\sigma_n^2}{\|\mathbf{a}(\boldsymbol{\alpha})\|^2 \sigma_s^2}\right) \text{CRB}_{\text{det}}(\boldsymbol{\alpha}) = [\mathbf{F}(\boldsymbol{\alpha})]^{-1} \tag{4}$$

where

$$\mathbf{F}(\boldsymbol{\alpha}) = c_\sigma(\boldsymbol{\alpha}) \text{Re}\left[\|\mathbf{a}(\boldsymbol{\alpha})\|^2 \mathbf{D}^H(\boldsymbol{\alpha})\mathbf{D}(\boldsymbol{\alpha}) - \mathbf{D}^H(\boldsymbol{\alpha})\mathbf{a}(\boldsymbol{\alpha})\mathbf{a}^H(\boldsymbol{\alpha})\mathbf{D}(\boldsymbol{\alpha})\right]$$

with $\mathbf{D}(\boldsymbol{\alpha}) \stackrel{\text{def}}{=} \left[\frac{\partial \mathbf{a}(\boldsymbol{\alpha})}{\partial \alpha_1}, ..., \frac{\partial \mathbf{a}(\boldsymbol{\alpha})}{\partial \alpha_L}\right]$ and where $c_\sigma(\boldsymbol{\alpha}) \stackrel{\text{def}}{=} \frac{2N\sigma_s^4}{\sigma_n^2(\sigma_n^2 + \|\mathbf{a}(\boldsymbol{\alpha})\|^2 \sigma_s^2)}$ is independent of the source and sensors positions for constant modulus steering vectors, only.

Thanks to (4), we only consider the stochastic source model for which the elements of the matrix $\mathbf{F}$ (**??**) are given by

$$\begin{aligned} \frac{[\mathbf{F}]_{i,j}}{c_\sigma(\boldsymbol{\alpha})} &= \left(\sum_{p=1}^{P} g_p^2\right)\left(\sum_{p=1}^{P} g'_{p,i} g'_{p,j} + \tau'_{p,i}\tau'_{p,j} g_p^2\right) - \left(\sum_{p=1}^{P} g'_{p,i} g_p\right)\left(\sum_{p=1}^{P} g'_{p,j} g_p\right) \\ &- \left(\sum_{p=1}^{P} \tau'_{p,i} g_p^2\right)\left(\sum_{p=1}^{P} \tau'_{p,j} g_p^2\right) \end{aligned} \tag{6}$$

where $g'_{p,i}$ and $\tau'_{p,i}$ are the derivative of g_p and τ_p w.r.t. α_i, respectively.

This expression simplifies when the gain g_p does not depend on the sensor ($g_p = g(\boldsymbol{\alpha})$) for which the following expression holds:

$$\frac{[\mathbf{F}]_{i,j}}{c'_\sigma(\boldsymbol{\alpha})} = P\sum_{p=1}^{P} \tau'_{p,i}\tau'_{p,j} - \left(\sum_{p=1}^{P} \tau'_{p,i}\right)\left(\sum_{p=1}^{P} \tau'_{p,j}\right) \tag{7}$$

where now $c'_\sigma(\boldsymbol{\alpha}) \stackrel{\text{def}}{=} \frac{2N\sigma_s^4 g^4(\boldsymbol{\alpha})}{\sigma_n^2(\sigma_n^2 + Pg^2(\boldsymbol{\alpha})\sigma_s^2)}$. Consequently the CRB ($\text{CRB}^{\text{DIR}}(\boldsymbol{\alpha})$) associated with directional sensors (with identical orientations and power profiles) is related to the CRB ($\text{CRB}^{\text{ISO}}(\boldsymbol{\alpha})$) associated with isotropic (i.e., omnidirectional with no power profile, $g_p = 1$) sensors by the following relation:

$$\text{CRB}^{\text{DIR}}(\boldsymbol{\alpha}) = \frac{1}{g^4(\boldsymbol{\alpha})} \frac{1 + Pg^2(\boldsymbol{\alpha})\frac{\sigma_s^2}{\sigma_n^2}}{1 + P\frac{\sigma_s^2}{\sigma_n^2}} \text{CRB}^{\text{ISO}}(\boldsymbol{\alpha}). \tag{8}$$

Note that this theoretical relation does no apply in practice for directional sensors in the near filed because...

B. Taylor expansion of the near-field matrix $\mathbf{F}$

In the addressed problem, $\alpha_1 = \theta$ and $\alpha_2 = r$. To obtain interpretable closed-form expressions of the CRB on θ and r, we consider a unitary modulus gain for each sensor,[2] as often assumed in the

[2]This condition, stronger than $\|\mathbf{a}(\boldsymbol{\alpha})\|^2 = P$ can be extended to arbitrary common gain $g(\boldsymbol{\alpha})$ thanks to (8).

CRB literature, for which $c'_\sigma(\boldsymbol{\alpha})$ simplifies to $c_\sigma = \frac{2N\sigma_s^4}{\sigma_n^2(\sigma_n^2+P\sigma_s^2)}$, independent of the source and sensors positions.

The following Taylor expansion of the matrix $\mathbf{F}$ (7) is proved in Appendix A:

$$\frac{2c}{r\cos^3(\theta)}[\mathbf{F}]_{1,2} = P\frac{S_3}{r^3} + \sin(\theta)\frac{3PS_4 - S_2^2}{r^4} + o(\epsilon^4) \quad (9)$$

$$\frac{c}{r^2\cos^2(\theta)}[\mathbf{F}]_{1,1} = P\frac{S_2}{r^2} + 2P\sin(\theta)\frac{S_3}{r^3} + \frac{S_4P\left[4\sin^2(\theta)-1\right] - S_2^2\sin^2(\theta)}{r^4} + o(\epsilon^4), \quad (10)$$

$$\frac{c}{\cos^4(\theta)}[\mathbf{F}]_{2,2} = \frac{1}{4}\frac{PS_4 - S_2^2}{r^4} + \frac{PS_5 - S_2S_3}{r^5}\sin(\theta) + \frac{PS_6\left[23\sin^2(\theta)-3\right] - 3S_2S_4\left[5\sin^2(\theta)-1\right] - 8S_3^2\sin^2(\theta)}{8r^6} + o(\epsilon^6), \quad (11)$$

where $\epsilon \stackrel{\text{def}}{=} \frac{1}{r}\max_p|x_p|$, $\lim_{\epsilon\to 0} o(\epsilon)/\epsilon = 0$, $c \stackrel{\text{def}}{=} \frac{\lambda^2}{4\pi^2 c_\sigma}$ and $S_k \stackrel{\text{def}}{=} \sum_{p=1}^P x_p^k$ are array geometry dependent constants, with, in particular, $S_1 = 0$.

C. Taylor expansion of the near-field CRB

From the expression (9) of the matrix $\mathbf{F}$, we see that DOA and range are decoupled to the second-order in ϵ if and only if $S_3 = 0$. Consequently, the DOA and range estimates given by any efficient algorithm are uncorrelated to the second order in ϵ, if and only if $S_3 = 0$. This special, yet important case, will be studied in Sec. IV. For the moment, we give results about the general case of antenna arrays for which $S_3 \neq 0$.

From the matrix $\mathbf{F}$ given by (9), (10) and (11), the following expressions of the CRB on the DOA and range are proved in Appendix B.

$$\mathrm{CRB}(\theta) = \frac{c}{P}\frac{1}{S_2 - \frac{PS_3^2}{PS_4 - S_2^2}}\frac{1+\gamma_1\frac{\sin(\theta)}{r}}{\cos^2(\theta)} + o(\epsilon), \quad (12)$$

$$\frac{\mathrm{CRB}(r)}{r^4} = \frac{4c}{PS_4 - S_2^2 - P\frac{S_3^2}{S_2}}\frac{1+\gamma_2\frac{\sin(\theta)}{r}}{\cos^4(\theta)} + o(\epsilon), \quad (13)$$

where $\gamma_1 \stackrel{\text{def}}{=} 4PS_3\frac{S_2S_3^2 - S_2^2S_4 + PS_4^2 - PS_3S_5}{(PS_4 - S_2^2)(PS_2S_4 - S_2^3 - PS_3^2)}$ and $\gamma_2 \stackrel{\text{def}}{=} 2\frac{3PS_2S_3S_4 + S_2^2S_3 - PS_3^3 - 2PS_2^2S_5}{S_2(PS_2S_4 - S_2^3 - PS_3^2)}$. Both depend on S_2, S_3, S_4 and S_5, but not on S_6.

D. The case of centro-symmetric arrays

Note that if $S_3 = 0$ [resp., if $S_3 = S_5 = 0$], the expression (12) [resp., (13)] is still valid. However, the term in $1/r$ in (12) of $\mathrm{CRB}(\theta)$ [resp., in (13) of $\mathrm{CRB}(r)$] vanishes. This scenario is far from being marginal, as it notably includes the ULA. Specific results are developed to cover such arrays. We will

discuss, in particular, the so-called *centro-symmetric* arrays, ones for which if a sensor is placed at some position x_p, then another one is placed at coordinate $-x_p$.

First, we prove that for antenna arrays with $S_3 = 0$ we have

$$\mathrm{CRB}(\theta) = c\frac{1 + \left[1 + \left(1 + \frac{4PS_4}{PS_4 - S_2^2}\right)\sin^2(\theta)\right]\frac{S_4}{S_2}\frac{1}{r^2}}{\cos^2(\theta)PS_2} + o(\epsilon^2). \tag{14}$$

Second, for antenna arrays that satisfy both $S_3 = 0$ and $S_5 = 0$, we prove that

$$\frac{\mathrm{CRB}(r)}{r^4} = c\frac{1}{\cos^4(\theta)}\frac{4}{PS_4 - S_2^2}\left[1 + \frac{\gamma_3(\theta)}{2(PS_4 - S_2^2)r^2}\right] + o(\epsilon^2), \tag{15}$$

where $\gamma_3(\theta) \stackrel{\text{def}}{=} \frac{18P^2S_4^2 + 2S_2^4 + 3PS_2^2S_4 - 23P^2S_2S_6}{PS_2}\sin^2(\theta) + 3PS_6 - 3S_2S_4$. The proofs are summarized in Appendix C.

E. Numerical validation

Let us, first, highlight similarities between the different obtained CRBs (12), (13), (14) and (15). For this purpose we define $C_1 \stackrel{\text{def}}{=} \frac{1}{c}\mathrm{CRB}(\theta)$ and $C_2 \stackrel{\text{def}}{=} \frac{1}{cr^4}\mathrm{CRB}(r)$, which also have the advantage of not depending on the noise and signal power, nor on the signal wavelength. They are purely geometrical functions of alone sensors and source positions.

For arbitrary linear arrays, (12) and (13) can be rewritten using the unique expression

$$C_i = \frac{T_i^{(1)}}{\cos^{2i}(\theta)}\left[1 + T_i^{(2)}\frac{\sin(\theta)}{r}\right] + o(\epsilon) \tag{16}$$

Expressions of constants $T_i^{(1)}$ and $T_i^{(2)}$ can be easily found and depend only on the array sensor positions. For centro-symmetric arrays (more explicitly, for arrays satisfying $S_3 = 0$ for C_1 and $S_3 = S_5 = 0$ for C_2), unified expressions can be found as well. Indeed, (14) and (15) are rewritten as a unique expression

$$C_i = \frac{T_i^{(3)}}{\cos^{2i}(\theta)}\left[1 + \left(T_i^{(4)}\sin^2(\theta) + T_i^{(5)}\right)\frac{T_i^{(6)}}{r^2}\right] + o(\epsilon^2) \tag{17}$$

where constants $T_i^{(3)}$ and $T_i^{(4)}$ can be easily verified to depend only on the array sensors positions. We intend to validate every single coefficient in the Taylor expansions in (12), (13), (14) and (15).

First, for arbitrary linear arrays, for $i = 1, 2$, we define $\rho_{1,i} \stackrel{\text{def}}{=} \frac{\cos^{2i}(\theta)C_i}{T_i^{(1)}}$ and $\rho_{2,i} \stackrel{\text{def}}{=} r\frac{\frac{\cos^{2i}(\theta)C_i}{T_i^{(1)}} - 1}{T_i^{(2)}\sin(\theta)}$. All converge to 1 when $1/\epsilon = r/\max_p |x_p|$ converges to infinity. This is verified in Fig. 2(a) that represents a randomly chosen linear array (for which $S_2 = 0.3162$ and $S_3 = 0.0904$) and source.

Second, for centro-symmetric arrays, for $i = 1, 2$, we introduce $\rho'_{1,i} \stackrel{\text{def}}{=} \frac{\cos^{2i}(\theta)C_i}{T_i^{(3)}}$ and $\rho'_{2,i} \stackrel{\text{def}}{=} r^2\frac{\frac{\cos^{2i}(\theta)C_i}{T_i^{(3)}} - 1}{\left(T_i^{(4)}\sin^2(\theta) + T_i^{(5)}\right)T_i^{(6)}}$, which, also, converge to 1 when $1/\epsilon = r/\max_p |x_p|$ converges to infinity. This is confirmed by the numerical evaluations for the 6 sensors ULA, reported in Fig. 2(b).

IV. Analysis of Centro-Symmetric Arrays

A. Centro-symmetric vs. non-centro-symmetric arrays

CRB expressions (12)-(13) as opposed to CRB expressions (14)-(15) suggest that there are two classes of antenna arrays with different geometrical properties and estimation performance. In particular, we are interested in the so-called centro-symmetric arrays because they have a better far-field estimation performance. To highlight this fact, we connect our near-field DOA CRB (12) and (14) to the stochastic far-field DOA CRB. The latter is given, for arbitrary linear arrays, by [7, rel. (5)]

$$\mathrm{CRB}_{\mathrm{FF}}(\theta) = \frac{1}{N} \frac{\lambda^2}{8\pi^2 \cos^2(\theta) \frac{S_2}{P} \frac{\sigma_s^2}{\sigma_n^2}} \left(1 + \frac{1}{P \frac{\sigma_s^2}{\sigma_n^2}}\right) = \frac{c}{\cos^2(\theta) P S_2}. \tag{18}$$

Normalized to the above, our near-field DOA CRBs (12) and (14) lead to, respectively,

$$\frac{\mathrm{CRB}(\theta)}{\mathrm{CRB}_{\mathrm{FF}}(\theta)} = \frac{1}{1 - \frac{PS_3^2}{PS_2S_4 - S_2^3}} \left[1 + \frac{\gamma_1 \sin(\theta)}{r} + o(\epsilon)\right], \tag{19}$$

$$\frac{\mathrm{CRB}(\theta)}{\mathrm{CRB}_{\mathrm{FF}}(\theta)} = 1 + \left[\sin^2(\theta)\left(1 + \frac{4PS_4}{PS_4 - S_2^2}\right) + 1\right] \frac{S_4}{S_2} \frac{1}{r^2} + o(\epsilon^2). \tag{20}$$

From (20), we see that arrays for which $S_3 = 0$ (e.g., for centro-symmetric arrays) do achieve $\mathrm{CRB}_{\mathrm{FF}}(\theta)$ when the source-to-array distance tends to infinity. At the same time, estimation of θ and r are decoupled in the matrix $\mathbf{F}$ to the second-order in ϵ. In contrast, non-centro-symmetric arrays in (19), for which $S_3 \neq 0$, verify $\lim_{r\to\infty} \mathrm{CRB}(\theta) > \mathrm{CRB}_{\mathrm{FF}}(\theta)$ because $PS_4 - S_2^2 > 0$ (see Sec. IV-C). This strange behavior is explained by the coupling between θ and r in the matrix $\mathbf{F}$ to the second-order in ϵ [see (9)]. More precisely, in the former case, the square of $[\mathbf{F}]_{1,2}$ tends to zero more rapidly than $[\mathbf{F}]_{2,2}$ when r tends to ∞, in contrast to the latter case for which the square of $[\mathbf{F}]_{1,2}$ and the term $[\mathbf{F}]_{2,2}$ tend to zero with the same speed. Consequently, from a practical point of view, as far as only the DOA parameter is considered, the far-field model of propagation, although approximative may be preferable to the exact near-field model for non centro-symmetric arrays with $S_3 \neq 0$.

If we take the range into consideration, the domain of validity of our approximations is larger for centro-symmetric arrays than for arbitrary arrays, as a result of a convergence in $1/r^2$ compared to $1/r$. Furthermore, when comparing (14) (15) to (12) (13), we realize that, for centro-symmetric arrays, the CRBs are symmetric w.r.t. positive/negative θ. However, for arbitrary arrays, they are not.

To illustrate the different behavior of centro-symmetric and non centro-symmetric arrays in the near-field region, we test in Fig. 3 antenna arrays of $P = 4$ sensors forming either (i) a ULA with a constant inter-sensors spacing d and for which $S_3 = S_5 = 0$, or (ii) a minimum hole and redundancy linear array (MHRLA) with inter-spacings d, $3d$, $2d$ [12] and for which $S_3 \neq 0$. Thanks to a larger aperture, the

MHRLA exhibits a lower far-field CRB, for instance, $\mathrm{CRB}_{\mathrm{FF}}^{\mathrm{MHRLA}}(\theta)/\mathrm{CRB}_{\mathrm{FF}}^{\mathrm{ULA}}(\theta) \approx 0.22$. However, due to the coupling of θ and r in the matrix $\mathbf{F}$ of the MHRLA, we have $\lim_{r\to\infty} \mathrm{CRB}(\theta) > \mathrm{CRB}_{\mathrm{FF}}(\theta)$ for this array. Furthermore, this figure confirms that the domain of validity of our approximations is much larger for the centro-symmetric than for non centro-symmetric arrays.

Finally, notice that because we fix the time reference at the centroid of the array (and not at the left-end as in [5]), we obtain simple and much easier to interpret closed-form CRB expressions that contrast with the intricate expressions [5, (10-11)] that are valid for the only ULA. In particular, we note the monotone behavior of $\mathrm{CRB}(\theta)$ w.r.t. r and the symmetry of $\mathrm{CRB}(\theta)$ and $\mathrm{CRB}(r)$ w.r.t. positive/negative θ with a minimum for $\theta = 0$. Also notice that, due to the change of time reference, our definition of the couple (θ, r) is different from the one in [5] (it is, actually, significantly different if the source is in the very near-field region).

B. Conditions of centro-symmetry

By centro-symmetric, we mean that the array is made of pairs of sensors placed at opposite coordinates, i.e., if a sensor is placed at x_p, then another one is placed at $-x_p$. A sensor may be placed at the origin and, then, P is odd. We determine that an array is centro-symmetric iff

$$S_i = 0 \text{ for all } i \text{ odd and less or equal to } P$$

This is proved by induction (see details in Appendix D) thanks to the Newton-Girard formula [16, pp. 69-74] that allows one to calculate the different S_i in an iterative manner.

C. Key geometric parameters for near-field performance

The rewriting of (12-15) allows us to point out two geometric parameters that shape the near-field accuracy of antenna arrays. They are the unit-less

$$\kappa \stackrel{\mathrm{def}}{=} \frac{S_2^2}{PS_4} \quad \text{and} \quad \eta \stackrel{\mathrm{def}}{=} \frac{S_2^3}{P^2 S_6}$$

which remain unchanged if either a sensor is added/removed at/from the origin, or, more importantly, if sensor coordinates are scaled by the same constant[3]. Before showing where κ and η appear in the CRB expressions and how they impact them, we highlight some of their intrinsic properties. First, we prove in Appendix E that

$$\eta \leq \kappa \leq 1. \tag{21}$$

[3]This property is useful to conduct an affordable systematic search of linear arrays under the non-restrictive condition $S_2 = 1$.

Very interesting is the fact that there is (almost) a one-to-one correspondence between κ and η. In fact, we prove in Appendix F that

$$\text{For } P=4: \eta=\eta_1(\kappa) \stackrel{\text{def}}{=} \frac{1}{\frac{3}{\kappa}-2} \quad \text{if} \quad S_1=S_3=0 \tag{22}$$

$$\text{For } P=5: \eta=\eta_2(\kappa) \stackrel{\text{def}}{=} \frac{4}{5\left(\frac{3}{\kappa}-\frac{5}{2}\right)} \quad \text{if} \quad S_1=S_3=S_5=0. \tag{23}$$

For larger P, the two functions [especially $\eta_2(\kappa)$] provide good approximations of the exact η, as validated by Fig. 4.

D. CRB in terms of κ and η

The two CRBs in (14) and (15) can now be rewritten as follows

$$\text{CRB}(\theta) = c\frac{\frac{1}{S_2}+\frac{1}{\kappa}\left[\left(1+\frac{4}{1-\kappa}\right)\sin^2(\theta)+1\right]\frac{1}{Pr^2}}{\cos^2(\theta)P}+o(\epsilon^2) \tag{24}$$

$$\frac{\text{CRB}(r)}{r^4} = c\frac{1}{\cos^4(\theta)}\frac{4}{S_2^2}\left[\frac{1}{\frac{1}{\kappa}-1}+\frac{S_2}{2Pr^2}\frac{\left(18+3\kappa+2\kappa^2-\frac{23}{\eta}\right)\sin^2(\theta)+3\frac{\kappa^2}{\eta}-3\kappa}{(1-\kappa)^2}\right]+o(\epsilon^2). \tag{25}$$

It becomes clear that while the array far-field (DOA estimation) performance is determined by S_2 only [which concurs with (18)], κ and η play a role in the (DOA and range estimation) near-field performance.

If S_2 is fixed (which has no impact on κ and η), and if we consider the most significant terms[4] of, respectively, (25) and (24), then it becomes clear that the array estimation performance is controlled by κ through, respectively, (i) $1/(1/\kappa-1)$ (an increasing function of κ) and (ii) function $f_\theta(\kappa)$ defined as

$$\begin{aligned} f_\theta(\kappa) &\stackrel{\text{def}}{=} \frac{1}{\kappa}\left[\left(1+\frac{4}{1-\kappa}\right)\sin^2(\theta)+1\right] \\ &\stackrel{\text{def}}{=} f_1(\kappa)\sin^2(\theta)+f_2(\kappa) \end{aligned}$$

The behavior of $f_\theta(\kappa)$, illustrated in Fig. 5, suggests that, for DOA estimation, an antenna with κ loosely close to $1/2$ ensures limited degradation in all look directions. Values of κ close to, but lower than, $1/2$ are preferred however, because they also lead to better estimation of the range parameter.

E. Comparison with ULA

The present analysis shows that, if the source is in the near-field of the linear antenna, then placing the sensors at a regular spacing will not ensure the best performance. For instance, we prove in Appendix G

[4]The first term is the most significant term in (25), for all configurations where $\frac{S_2}{2Pr^2}<0.01$, which covers a large domain of practical situations.

that, in the case of ULA, κ tends to $5/9$ (and η converges to $7/27$) if the number of sensors increases to infinity, which, by the way, leads to the following refinements of (24) and (25)

$$\mathrm{CRB}(\theta) \approx \mathrm{CRB}_{\mathrm{FF}}(\theta)\left\{1+\frac{3P^2d^2}{20r^2}\left[1+10\sin^2(\theta)\right]+o\left(\frac{P^2d^2}{r^2}\right)\right\}, \tag{26}$$

$$\frac{\mathrm{CRB}(r)}{r^4} \approx \frac{720c}{P^6d^4\cos^4(\theta)}\left\{1+\frac{9P^2d^2}{28r^2}\left[1-\frac{970}{27}\sin^2(\theta)\right]+o\left(\frac{P^2d^2}{r^2}\right)\right\}, \tag{27}$$

where d denotes the spacing between two consecutive sensors.

From the discussion in Sec. IV-D, a (centro-symmetric) linear antenna with such a value of κ has near-optimum performance for DOA estimation but not for range estimation. To better illustrate the impact of κ on the estimation performance (of both DOA and range), we compare the 6-sensors ULA (with sensors placed at ± 0.1195, ± 0.3586 and ± 0.5976) against a non-ULA array of 6 sensors located at ± 0.0674, ± 0.2023 and ± 0.6742. Both arrays exhibit the same $S_2 = 1$ (and, hence, have identical far-field DOA estimation CRBs). However, κ is equal to 0.5776 for the ULA and to 0.4 for the non-ULA. In Fig. 6, we report the ratios $\frac{\mathrm{CRB}(\theta)|_{\mathrm{non-ULA}}}{\mathrm{CRB}(\theta)|_{\mathrm{ULA}}}$ and $\frac{\mathrm{CRB}(r)|_{\mathrm{non-ULA}}}{\mathrm{CRB}(r)|_{\mathrm{ULA}}}$, calculated using the exact CRB expressions and the approximate CRB expressions in (24) and (25). There, we can see that while we obtain similar DOA performance, the non-ULA array has better range estimation capabilities. Hence, within the family of centro-symmetric linear arrays characterized by a given size P and a given value of S_2, all verify $\lim_{r\to\infty}\frac{\mathrm{CRB}(\theta)|_{\mathrm{non-ULA}}}{\mathrm{CRB}(\theta)|_{\mathrm{ULA}}} = 1$, from (24). However, from (25), the κ-dependent function

$$\mathcal{R}_P(\kappa) \overset{\mathrm{def}}{=} \lim_{r\to\infty}\frac{\mathrm{CRB}(r)|_{\mathrm{non-ULA}}}{\mathrm{CRB}(r)|_{\mathrm{ULA}}} = \frac{\frac{1}{\kappa_{\mathrm{ULA}}}-1}{\frac{1}{\kappa}-1}$$

can be seen as an indicator of improvement (over the ULA) whenever it is lower than one. For instance, if $P \gg 1$,

$$\mathcal{R}_P(\kappa) = \frac{4}{5}\frac{1}{\frac{1}{\kappa}-1}.$$

The above ratio is illustrated in Fig. 7 for the domain[5] $[0.3, 0.7]$ of κ outside which DOA near-field performance degrades severely (as clear from Fig. 5(c)). It can be seen from Fig. 7 that the (far-field) range CRB can be reduced by a much as 50% by antenna arrays with a κ moderately lower than that of the ULA.

[5]In fact, extreme values of κ (i.e. 0 and 1) are achieved by impractically co-localized sensors, either at the origin, or at the same distance (and on both sides) from the origin.

V. Conclusion

Assuming no constraints other than sensors deployed along a straight line and using the exact expression of the time delay parameter, accurate, simple and interpretable closed-form CRB expressions have been obtained for both angle and range parameters of a near-field narrow-band source.

They show the exact geometric condition for the antenna array to have an attractive behavior in its near-field: better precision and faster convergence to the lower far-field DOA CRB. Such a class of centro-symmetric arrays includes, but is not restricted to, ULAs. Furthermore, it is proved that appropriately designed centro-symmetric non-ULA can largely improve the range estimates without deteriorating the DOA estimates under near-field conditions. Because they potentially have better estimation performance, non-ULAs geometries may be adopted when array ambiguity can be tolerated or counter-measures are made available [7]. Hence, our analysis gives a deeper insight into the array near-field performance and shows that more flexibility is available for array design.

Appendix

A. Taylor expansion of the matrix $\mathbf{F}$: Proof of (9), (10) and (11)

The main steps of the proof are as follows. First, note that with $\epsilon_p \stackrel{\text{def}}{=} x_p/r$, we have

$$\begin{aligned}
\frac{\lambda}{2\pi}\sum_{p=1}^{P}\tau'_{p,1} &= \sum_{p=1}^{P}\cos(\theta)r\epsilon_p/\sqrt{\beta_p},\\
\frac{\lambda}{2\pi}\sum_{p=1}^{P}\tau'_{p,2} &= P+\sin(\theta)\sum_{p=1}^{P}\frac{\epsilon_p}{\sqrt{\beta_p}}-\sum_{p=1}^{P}\frac{1}{\sqrt{\beta_p}},\\
\frac{\lambda^2}{4\pi^2}\sum_{p=1}^{P}(\tau'_{p,1})^2 &= r^2\cos^2(\theta)\sum_{p=1}^{P}\frac{\epsilon_p^2}{\beta_p},\\
\frac{\lambda^2}{4\pi^2}\sum_{p=1}^{P}(\tau'_{p,2})^2 &= P+\sum_{p=1}^{P}\frac{\epsilon_p^2\sin^2(\theta)+1-2\epsilon_p\sin(\theta)}{\beta_p}+2\sum_{p=1}^{P}\frac{\epsilon_p\sin(\theta)-1}{\sqrt{\beta_p}}\\
\frac{\lambda^2}{4\pi^2}\sum_{p=1}^{P}\tau'_{p,1}\tau'_{p,2} &= r\cos(\theta)\sum_{p=1}^{P}\epsilon_p\left(\frac{1}{\sqrt{\beta_p}}+\frac{\epsilon_p\sin(\theta)-1}{\beta_p}\right).
\end{aligned}$$

All these sums appear to involve either $1/\beta$ or $1/\sqrt{\beta}$, whose Taylor expansions are obtained subsequently:

$$\begin{aligned}
\frac{1}{\beta_p} &= 1 + 2\epsilon_p \sin(\theta) + (4\sin^2(\theta) - 1)\epsilon_p^2 - 4\sin(\theta)\cos(2\theta)\epsilon_p^3 + (1 - 12\sin^2(\theta) + 16\sin^4(\theta))\epsilon_p^4 \\
&+ \sin(\theta)(6 - 32\sin^2(\theta) + 32\sin^4(\theta))\epsilon_p^5 + [-1 + 24\sin^2(\theta)1 - 80\sin^4(\theta) + 64\sin^6(\theta)]\epsilon_p^6 + o(\epsilon_p^6), \\
\frac{1}{\sqrt{\beta_p}} &= 1 + \epsilon_p \sin(\theta) + \frac{3\sin^2(\theta) - 1}{2}\epsilon_p^2 + \sin(\theta)\frac{5\sin^2(\theta) - 3}{2}\epsilon_p^3 + \frac{3 - 30\sin^2(\theta) + 35\sin^4(\theta)}{8}\epsilon_p^4 \\
&+ \sin(\theta)\frac{15 - 70\sin^2(\theta) + 63\sin^4(\theta)}{8}\epsilon_p^5 + \frac{-5 + 105\sin^2(\theta) - 315\sin^4(\theta) + 231\sin^6(\theta)}{16}\epsilon_p^6 + o(\epsilon_p^6).
\end{aligned}$$

The above expansions are used to obtain Taylor expansion of the different sums appearing in the right hand side of (7). After tedious manipulations, (9), (10) and (11) are obtained in similar fashions. ■

B. Taylor expansion of the CRB for arbitrary arrays: Proof of (12) and (13)

First, note that by replacing r by $\max_p |x_p|/\epsilon$ in the $[\mathbf{F}]_{i,j}$ terms (9-11), the matrix $\mathbf{F}$ can be written in the following form:

$$\mathbf{F} = \begin{bmatrix} b_0^{1,1} + b_1^{1,1}\epsilon + b_2^{1,1}\epsilon^2 + o(\epsilon^2) & b_2^{1,2}\epsilon^2 + b_3^{1,2}\epsilon^3 + o(\epsilon^3) \\ b_2^{1,2}\epsilon^2 + b_3^{1,2}\epsilon^3 + o(\epsilon^3) & \epsilon^4[b_4^{2,2} + b_5^{2,2}\epsilon + b_6^{2,2}\epsilon^2 + o(\epsilon^2)] \end{bmatrix},$$

where for e.g., $b_0^{1,1} = \frac{\cos^2(\theta)}{c} PS_2$. This allows one to obtain, after straightforward algebraic manipulations,

$$\begin{aligned}
\mathrm{CRB}(\theta) &= [\mathbf{F}^{-1}]_{1,1} = \frac{1}{b_0^{1,1} - \frac{(b_2^{1,1})^2}{b_4^{2,2}}} \left[1 + \epsilon\left(\frac{b_5^{2,2}}{b_4^{2,2}} - \frac{b_0^{1,1}b_5^{2,2} + b_1^{1,1}b_4^{2,2} - 2b_2^{1,2}b_3^{1,2}}{b_0^{1,1}b_4^{2,2} - (b_2^{1,1})^2}\right) + o(\epsilon)\right], \\
\mathrm{CRB}(r) &= [\mathbf{F}^{-1}]_{2,2} = \frac{1}{\epsilon^4 b_4^{2,2}\left(1 - \frac{(b_2^{1,1})^2}{b_0^{1,1}b_4^{2,2}}\right)} \left[1 + \epsilon\left(\frac{b_1^{1,1}}{b_0^{1,1}} - \frac{\frac{b_5^{2,2}}{b_4^{2,2}} + \frac{b_1^{1,1}}{b_0^{1,1}} - \frac{2b_2^{1,2}b_3^{1,2}}{b_0^{1,1}b_4^{2,2}}}{1 - \frac{b_2^{1,1}}{b_0^{1,1}b_4^{2,2}}}\right) + o(\epsilon)\right].
\end{aligned}$$

By replacing the different terms $b_k^{i,j}$ by their respective values, and after simple but tedious manipulations, we ultimately prove (12) and (13). ■

C. Taylor expansion of the CRB for centro-symmetric arrays: Proof of (14) and (15)

We use the same approach as in Sec. B. On one hand, we have, for $S_3 = 0$,

$$\mathbf{F} = \begin{bmatrix} b_0^{1,1} + b_2^{1,1}\epsilon^2 + o(\epsilon^2) & b_3^{1,2}\epsilon^3 + o(\epsilon^3) \\ b_3^{1,2}\epsilon^3 + o(\epsilon^3) & \epsilon^4[b_4^{2,2} + b_5^{2,2}\epsilon + b_6^{2,2}\epsilon^2 + o(\epsilon^2)] \end{bmatrix}.$$

which allows to conclude that

$$\mathrm{CRB}(\theta) = [\mathbf{F}^{-1}]_{1,1} = \frac{1}{b_0^{1,1}}\left[1 - \epsilon^2\left(\frac{b_2^{1,1}}{b_0^{1,1}} - \frac{(b_3^{1,2})^2}{b_0^{1,1}b_4^{2,2}}\right) + o(\epsilon^2)\right].$$

On the other hand, when both $S_3 = S_5 = 0$, we have

$$\mathbf{F} = \left[\begin{array}{cc} b_0^{1,1} + b_2^{1,1}\epsilon^2 + o(\epsilon^2) & b_3^{1,2}\epsilon^3 + o(\epsilon^3) \\ b_3^{1,2}\epsilon^3 + o(\epsilon^3) & \epsilon^4[b_4^{2,2} + b_6^{2,2}\epsilon^2 + o(\epsilon^2)] \end{array} \right],$$

which eventually leads to

$$\mathrm{CRB}(r) \;\; = \;\; [\mathbf{F}^{-1}]_{2,2} = \frac{1}{\epsilon^4 b_4^{2,2}} \left[1 - \epsilon^2 \left(\frac{b_6^{2,2}}{b_4^{2,2}} - \frac{(b_3^{1,3})^2}{b_0^{1,1} b_4^{2,2}} \right) + o(\epsilon^2) \right].$$

Replacing the different terms $b_k^{i,j}$ by their values, (14) and (15) are also proved after tedious manipulations. ■

D. Proof of the condition of centro-symmetry of Sec. IV-B

We consider real numbers $x_1, \cdots, x_P$ and form the polynomial $Q(x) \stackrel{\mathrm{def}}{=} (x - x_1) \cdots (x - x_P) \stackrel{\mathrm{def}}{=} x^P - \sigma_1 x^{P-1} + \sigma_2 x^{P-2} + \cdots + (-1)^P \sigma_P$. The coefficients $\sigma_1, \cdots, \sigma_P$, given by $\sigma_k \stackrel{\mathrm{def}}{=} \sum_{1 \leq i_1 < i_2 < \cdots < i_k \leq P} x_{i_1} x_{i_2} \cdots x_{i_k}$, are known to be linked to $S_1, \cdots, S_P$ defined as $S_k = \sum_{p=1}^P x_p^k$ by means of the Newton-Girard formula [16, pp. 69-74]

$$S_k = \sum_{l=1}^{k-1} (-1)^{l-1} \sigma_l S_{k-l} + (-1)^{k-1} k \sigma_k, k \geq 2 \tag{28}$$

where by definition $\sigma_{P+1} = \sigma_{P+2} = \cdots = 0$. Let $1, 3, \cdots, 2I+1$ be all the odd integers $\leq P$. Let's assume that $S_1 = S_3 = \cdots = S_{2I+1} = 0$. We will prove that $\sigma_1 = \sigma_3 = \cdots = \sigma_{2I+1} = 0$. We proceed by induction to show that $\sigma_{2i+1} = 0$ for $i = 0, 1, \cdots, I$. This is already verified for $i = 0$ because $\sigma_1 = S_1$. Let's assume $\sigma_1 = \sigma_3 = \cdots = \sigma_{2i+1} = 0$ for some $i \leq I$, and let's prove that $\sigma_{2i+3} = 0$. From (28), we have $S_{2i+3} = \sum_{l=1}^{2i+2} (-1)^{l-1} \sigma_l S_{2i+3-l} + (-1)^{2i+2} (2i+3) \sigma_{2i+3}$ is necessarily zero. In fact, $2i+3$ is odd, so that if l is odd, then $2i+3-l$ is even and vice versa, for $l = 1, \cdots, 2i+2$. Also, l and $2i+3-l$ both are $\leq 2i+1$ and whenever one is odd, the corresponding σ and S coefficients are zero. Hence, for $l = 1, \cdots, 2i+2$, we have necessarily $\sigma_l S_{2i+3-l} = 0$; and so is σ_{2i+3}. Finally, $Q(x)$ is either $x^P + \sigma_2 x^{P-2} + \sigma_4 x^{P-4} + \cdots + \sigma_P$ if P is even or $x^P + \sigma_2 x^{P-2} + \sigma_4 x^{P-4} + \cdots + \sigma_{P-1} x$ if P is odd. In the first (resp. second) case, zeros of $Q(x)$, i.e. $x_1, \cdots, x_P$, are of the form $\pm\alpha_1, \pm\alpha_2, \cdots$ (resp. $0, \pm\alpha_1, \pm\alpha_2, \cdots$). ■

E. Proof of inequalities (21)

For arbitrarily chosen $a_1 \leq a_2 \leq \cdots \leq a_P$ and $b_1 \leq b_2 \leq \cdots \leq b_P$, we have $\sum_{i=1}^P \sum_{j=1}^P (a_i - a_j)(b_i - b_j) \geq 0$ which implies that $P \sum_{i=1}^P a_i b_i \geq \left(\sum_{i=1}^P a_i \right) \left(\sum_{i=1}^P b_i \right)$, the so-called Tchebychev's sum inequality. If we let $a_i \stackrel{\mathrm{def}}{=} b_i \stackrel{\mathrm{def}}{=} x_i^2$, we obtain $P S_4 \geq S_2^2$ i.e. $\kappa \leq 1$. If we let $a_i \stackrel{\mathrm{def}}{=} x_i^2$ and $b_i \stackrel{\mathrm{def}}{=} x_i^4$, we obtain $P S_6 \geq S_2 S_4$ i.e. $\eta \leq \kappa$. ■

F. Proof of (22) and (23)

By virtue of (28), we have $S_2 = \sigma_1 S_1 - 2\sigma_2$, $S_4 = \sigma_1 S_3 - \sigma_2 S_2 + \sigma_3 S_1 - 4\sigma_4$ and $S_6 = \sigma_1 S_5 - \sigma_2 S_4 + \sigma_3 S_3 - \sigma_4 S_2 + \sigma_5 S_1 - 6\sigma_6$. If $S_1 = S_3 = S_5 = 0$ (if $P = 4$, only if $S_1 = S_3 = 0$, because this is sufficient to have a centro-symmetric array and automatically implies $S_5 = 0$), and after proper replacement, we obtain $S_6 = \frac{3S_2S_4}{4} - \frac{S_2^3}{8} - 6\sigma_6$ which can be transformed into $\frac{3}{\kappa} = \frac{4}{P}\frac{1}{\eta} + \frac{P}{2} + 24P\frac{\sigma_6}{S_2^3}$ By definition, $\sigma_6 = 0$ if $P < 6$ and the following becomes clearly justified

$$\begin{aligned} P = 4, S_1 = S_3 = 0 \quad &\rightarrow \quad \frac{3}{\kappa} = \frac{1}{\eta} + 2 \\ P = 5, S_1 = S_3 = S_5 = 0 \quad &\rightarrow \quad \frac{3}{\kappa} = \frac{4}{5}\frac{1}{\eta} + \frac{5}{2}. \end{aligned}$$

■

G. κ and η for large-sized ULAs

Consider a ULA centered at the origin made of P sensors spaced by d. The proof is given for odd $P = 2Q + 1$ (extension to even P can be conducted in a similar way). Using the identities of $\sum_{k=1}^{Q} k^\alpha$ for $\alpha = 2, 4$ and 6, we obtain

$$\begin{aligned} S_2 &= 2d^2 \sum_{k=1}^{Q} k^2 = d^2 \frac{Q(Q+1)(2Q+1)}{3} \\ S_4 &= 2d^4 \sum_{k=1}^{Q} k^4 = d^2 \frac{3Q^2 + 3Q - 1}{5} S_2 \\ S_6 &= 2d^6 \sum_{k=1}^{Q} k^6 = d^4 \frac{3Q^4 + 6Q^3 - 3Q + 1}{7} S_2, \end{aligned}$$

which directly implies

$$\kappa = \frac{S_2^2}{PS_4} = \frac{5}{3}\frac{Q(Q+1)}{3Q^2 + 3Q - 1} \quad \text{and} \quad \eta = \frac{S_2^3}{P^2 S_6} = \frac{7}{9}\frac{Q^2(Q+1)^2}{3Q^4 + 6Q^3 - 3Q + 1}.$$

■

REFERENCES

[1] H. Krim and M. Viberg, "Two decades of array signal processing research," *IEEE Signal Process. Mag.*, vol. 13, no. 4, pp. 67-94, Jul. 1996.

[2] H. Gazzah and S. Marcos, "Cramer-Rao bounds for antenna array design," *IEEE Trans. Signal Process.*, vol. 54, no. 1, pp. 336-345, Jan. 2006.

[3] E. Grosicki, K. Abed-Meraim, and Y. Hua, "A weighted linear prediction method for near field source localization," *IEEE Trans. Signal Process.*, vol. 53, no. 10, pp. 3651-3660, Oct. 2005.

[4] M. N. El Korso, R. Boyer, A. Renaux, and S. Marcos, "Conditional and unconditional Cramer Rao bounds for near-field Source localization," *IEEE Trans. Signal Process.*, vol. 58, no. 5, pp. 2901-2906, May 2010.

[5] Y. Begriche, M. Thameri, and K. Abed-Meraim, "Exact Cramer Rao bound for near field source localization," in *Proc. International Conference on Information Science, Signal Processing and their Applications*, 2012, pp. 718-721.

[6] Y. Begriche, M. Thameri, and K. Abed-Meraim, "Exact conditional and unconditional Cramer Rao bound for near field localization," in arXiv.

[7] C. ElKassis, J. Picheral, and C. Mokbel, "Advantages of nonuniform arrays using root-MUSIC", *Signal Processing*, Elsevier, vol. 90 (210), pp. 689-695.

[8] M. Gavish and A. J. Weiss, "Array geometry for ambiguity resolution in direction finding," *IEEE Trans. Antennas Propagat.*, vol. 39, pp. 143-146, Feb. 1991.

[9] A. J. Weiss, A. S. Willsky, and B. C. Levy, "Non uniform array processing via the polynomial approach," *IEEE Trans. Aerosp. Electron. Syst.*, vol. 25, no. 1, pp. 48-55, 1989.

[10] H. Gazzah and J.-P. Delmas, "Spectral efficiency of beamforming-based parameter estimation in the single source case," in *Proc. IEEE SSP*, Nice, pp. 153-156, 2011.

[11] J.-P. Delmas and H. Gazzah, "CRB Analysis of near-field source localization using uniform circular arrays," in *Proc. ICASSP*, Vancouver pp. 3396-3400, 2013.

[12] Y. Meurisse and J.P. Delmas, "Bounds for sparse planar and volume arrays," *IEEE Trans. Inform. Theory*, vol. 47, no. 1, pp. 464-468, January 2001.

[13] P. Stoica and A. Nehorai, "Performances study of conditional and unconditional direction of arrival estimation," *IEEE Trans. ASSP*, vol. 38, no. 10, pp. 1783-1795, Oct. 1990.

[14] H. Abeida, J.-P. Delmas, "Efficiency of subspace-based DOA estimators," *Signal Processing*, vol. 87, no. 9, pp. 2075-2084, Sept. 2007.

[15] D.T. Vu, A. Renaux, R. Boyer, and S. Marcos, "A Cramer Rao bounds based analysis of 3D antenna array geometries made from ULA branches," *Multidimensional Systems and Signal Processing, Springer*, Oct. 2011.

[16] L. E. Dickson, "Elementary Theory of Equations," New York, Wiley and Sons, 1914.

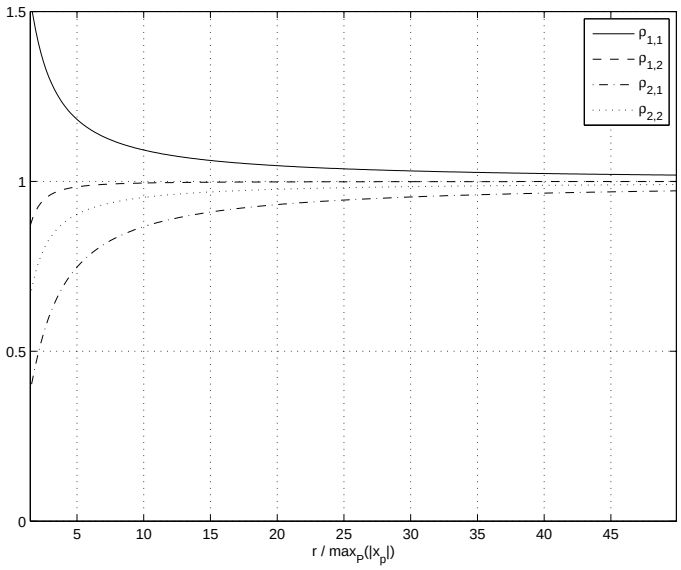

(a)

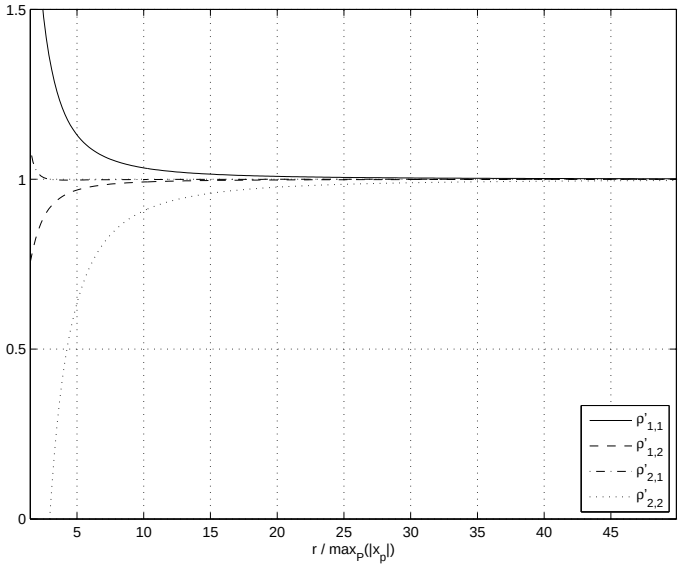

(b)

Fig. 2. Validation of the DOA and range CRBs for an increasing source-to-array distance. The array is made of 6 sensors. In (a), they are placed at -0.1672, -0.0737, 0.0960, -0.1444, 0.4694 and -0.1801, forming a non centro-symmetric array. In (b), they form a ULA. The source is placed, in (a), with $\theta = 47.13°$; and, in (b), with $\theta = 146.64°$.

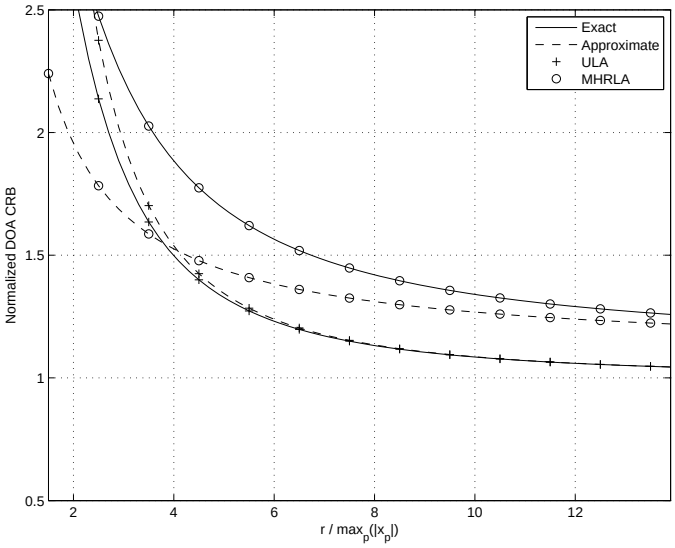

Fig. 3. Approximative and exact ratios $\mathrm{CRB}(\theta)/\mathrm{CRB}_{\mathrm{FF}}(\theta)$ for 4-sensors ULA and MHRLA and a source at $\theta = 60°$. Approximate ratios are calculated using (19) for the (non-centro-symmetric) MHRLA, and (20) for the (centro-symmetric) ULA.

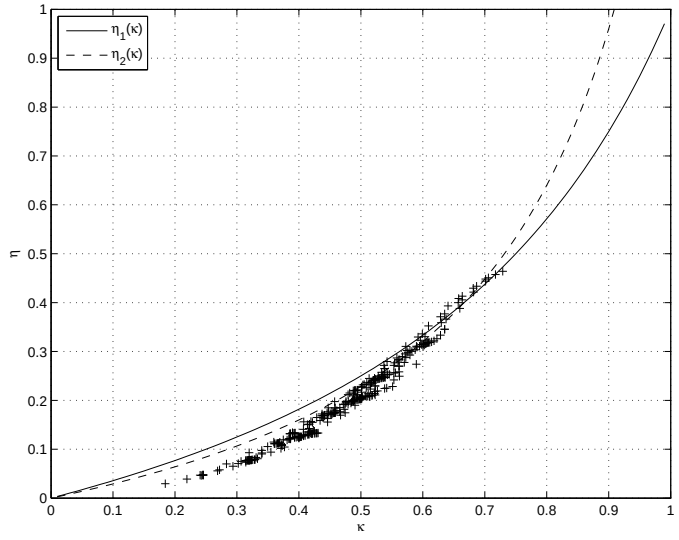

Fig. 4. Systematic search for centro-symmetrical arrays of $P = 15$ sensors verifying $S_2 = 1$. κ and η are reported as '+' dots; and so in comparison with $\eta_1(\kappa)$ and $\eta_2(\kappa)$.

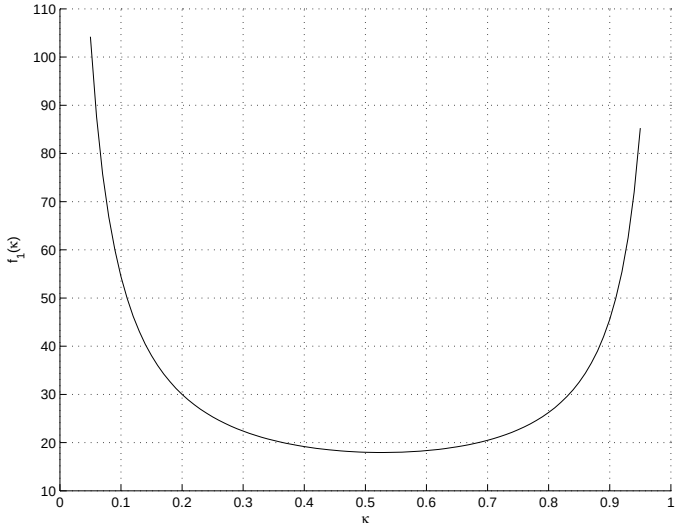

(a) $f_1(\kappa)$

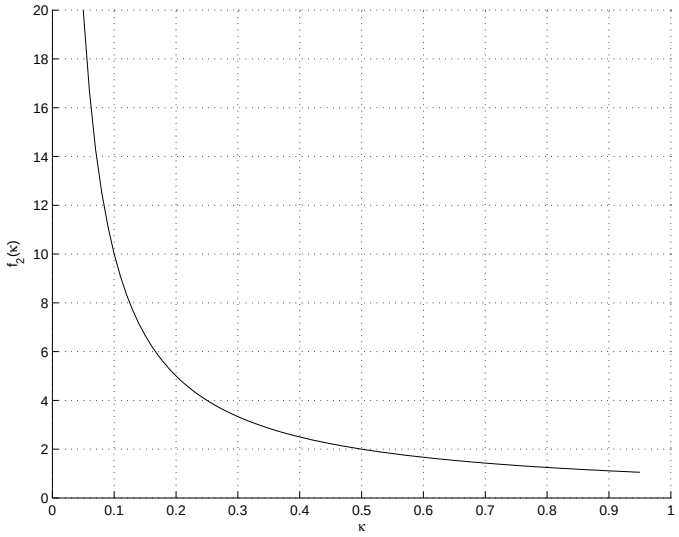

(b) $f_2(\kappa)$

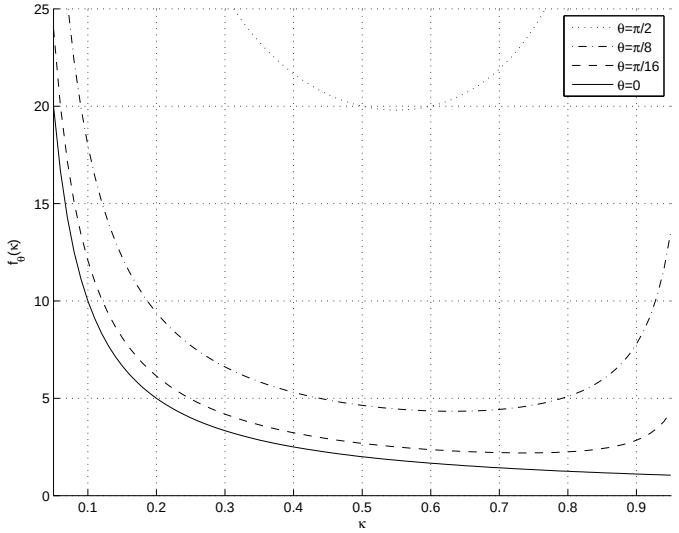

(c) $f_\theta(\kappa)$

Fig. 5. Near-field DOA estimation performance, expressed by $f_\theta(\kappa)$ [and its constituent functions $f_1(\kappa)$ and $f_2(\kappa)$], as function

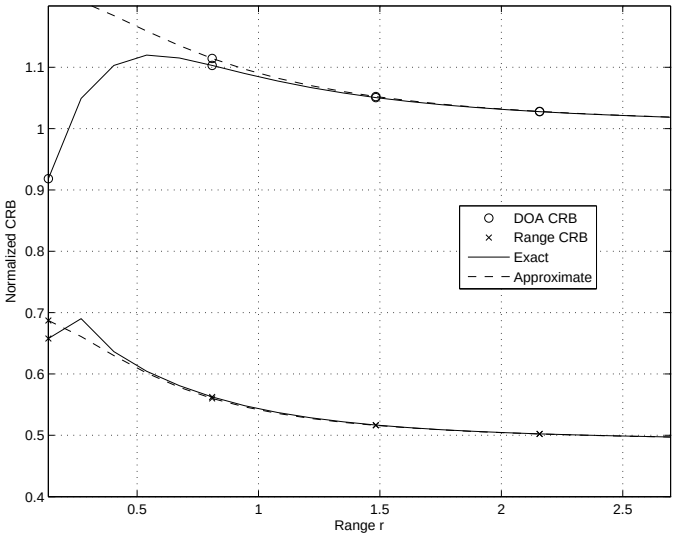

Fig. 6. DOA and range CRBs of the non-ULA ($\kappa = 0.4$) normalized to that of the equivalent ULA ($\kappa = 0.5776$). Both arrays are made of $P = 6$ sensors and are such that $S_2 = 1$.

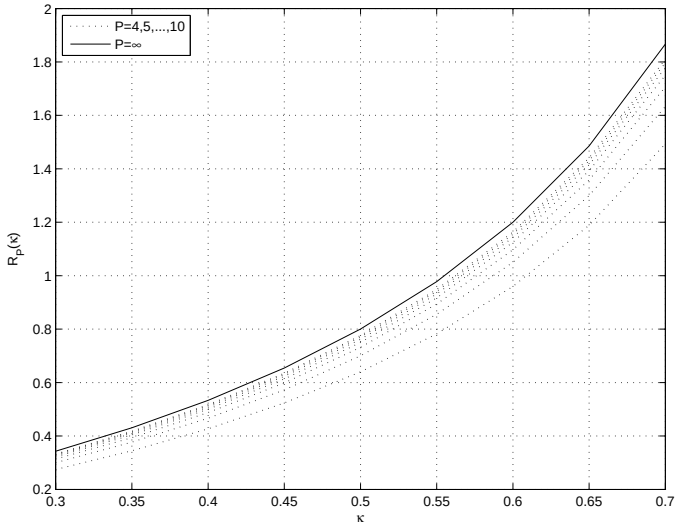

Fig. 7. Centro-symmetric non-ULA vs. ULA: Compared range estimation performance of far-field sources.